Supporting information for
CryoSeekV: Discovery of a novel virus AaTLV-IMCAS from *Aedes albopictus* cells by cryogenic electron microscopy

Hao Qu[a,b,1], Linjie Li[a,1], Xiaoming Li[a,c], Yunhan Xi[a,b], Ruirui Yang[a,d], Xiao Qu[a], Qiuyao Jiang [e], Peiyi Wang [f],Shihua Li[a,*] and George F. Gao[a,g,*]

[a] CAS Key Laboratory of Pathogen Microbiology and Immunology, Institute of Microbiology, Chinese Academy of Sciences (CAS), Beijing 100101, China;
[b] Medical School, University of Chinese Academy of Sciences (UCAS), Beijing 100101, China;
[c] Department of Gastroenterology, Shenzhen Children's Hospital, Shenzhen 518000, China;
[d] Shanxi Key Laboratory of Animal Disease Research, Prevention and Control, College of Veterinary Medicine, Shanxi Agricultural University, Jinzhong 030801, China;
[e] Medical Science and Technology Innovation Center, Shandong First Medical University & Shandong Academy of Medical Sciences, 250000 Jinan, China;
[f] Institute of Crop Microstructure Research, Shandong Agricultural University, Tian 271018, China;
[g] Institute of Viral Disease Control and Prevention, Chinese Center for Disease Control and Prevention (China CDC), Beijing 102206, China;
[1]H.Q. and L.L. contributed equally to this work.

Correspondence
George F. Gao, CAS Key Laboratory of Pathogen Microbiology and Immunology, Institute of Microbiology, Chinese Academy of Sciences, 100101 Beijing, China.
[*]**To whom correspondence may be addressed.** Email: lish@im.ac.cn or gaof@im.ac.cn.

This PDF file includes:

Supporting Information Text

Supplementary Figures

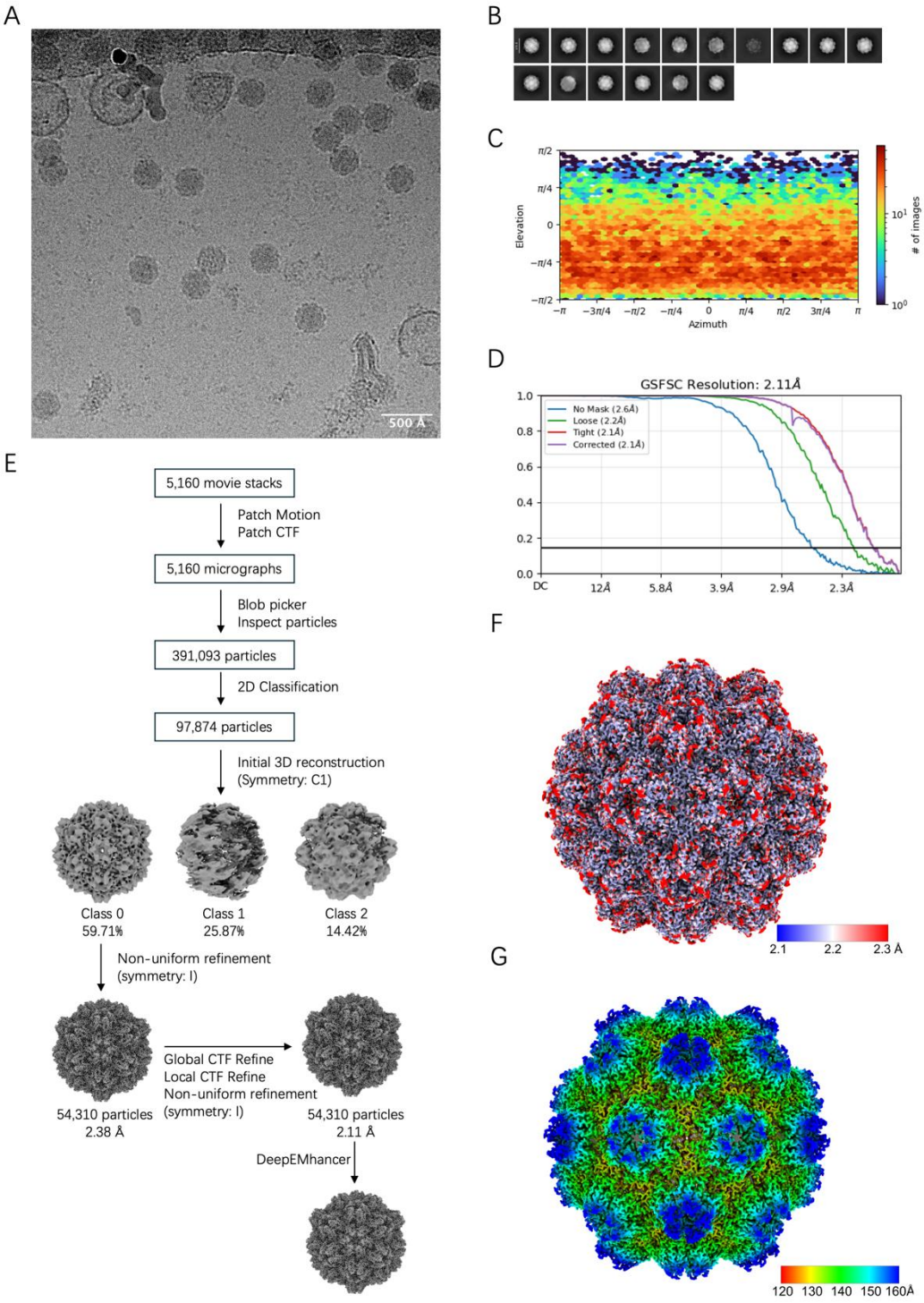

Fig. S1. Cryo-EM single-particle reconstruction and resolution evaluation of the AaTLV capsid. (A) Representative cryo-EM micrograph of AaTLV particles. Scale bar, 500 Å. (B) Representative reference-free 2D class averages showing distinct structural orientations of the icosahedral capsid. (C) Angular distribution of the particles included in the final 3D refinement. (D) Gold-standard Fourier shell correlation (FSC) curves of the final 3D reconstruction. (E) Schematic workflow of cryo-EM image processing and 3D reconstruction

in cryoSPARC. (F) Cryo-EM density map of the AaTLV capsid colored according to local resolution (ranging from 2.1 Å in blue to 2.3 Å in red) estimated in cryoSPARC. (G) Surface representation of the viral capsid colored radially according to distance from the particle center (120 Å to 160 Å).

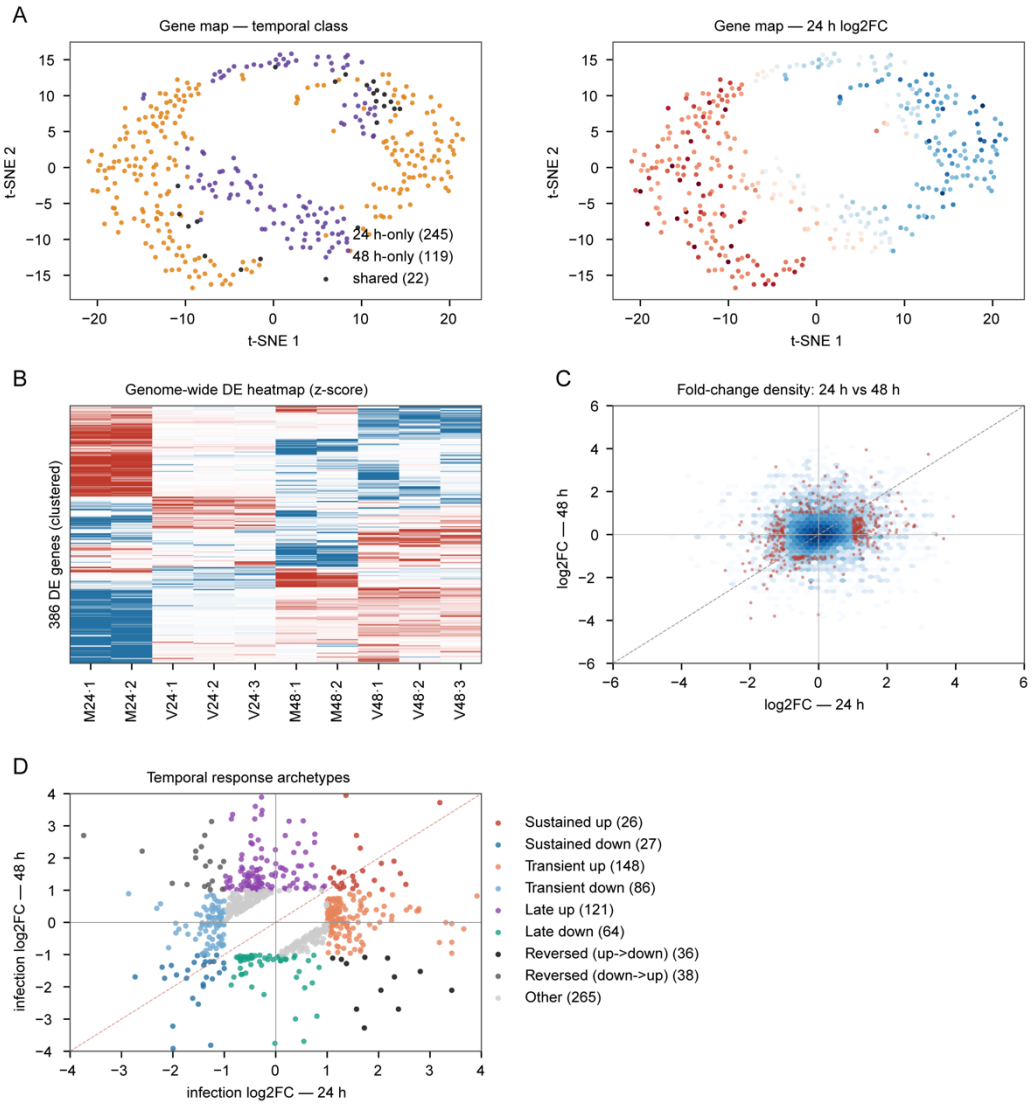

Fig. S2. Expression landscape and temporal structure. (A) t-SNE gene-expression map of the 386 DEGs coloured by temporal class (24 h-only, 48 h-only, shared; left) and by 24 h log2 fold change (right). (B) Hierarchically clustered heatmap of all DEGs across the ten libraries (row z-scores of log2-normalized counts; columns are samples ordered by group). (C) Hexbin density of gene-wise log2 fold changes at 24 h (x) versus 48 h (y) for all tested genes (blue density) with DEGs overlaid in red; the dashed line is the identity. (D) Temporal response archetypes: every DE gene plotted by infection log2 fold change at 24 h versus 48 h and coloured by archetype (sustained, transient, late and reversed up/down; counts given in the legend); the dashed diagonal marks a sustained response.

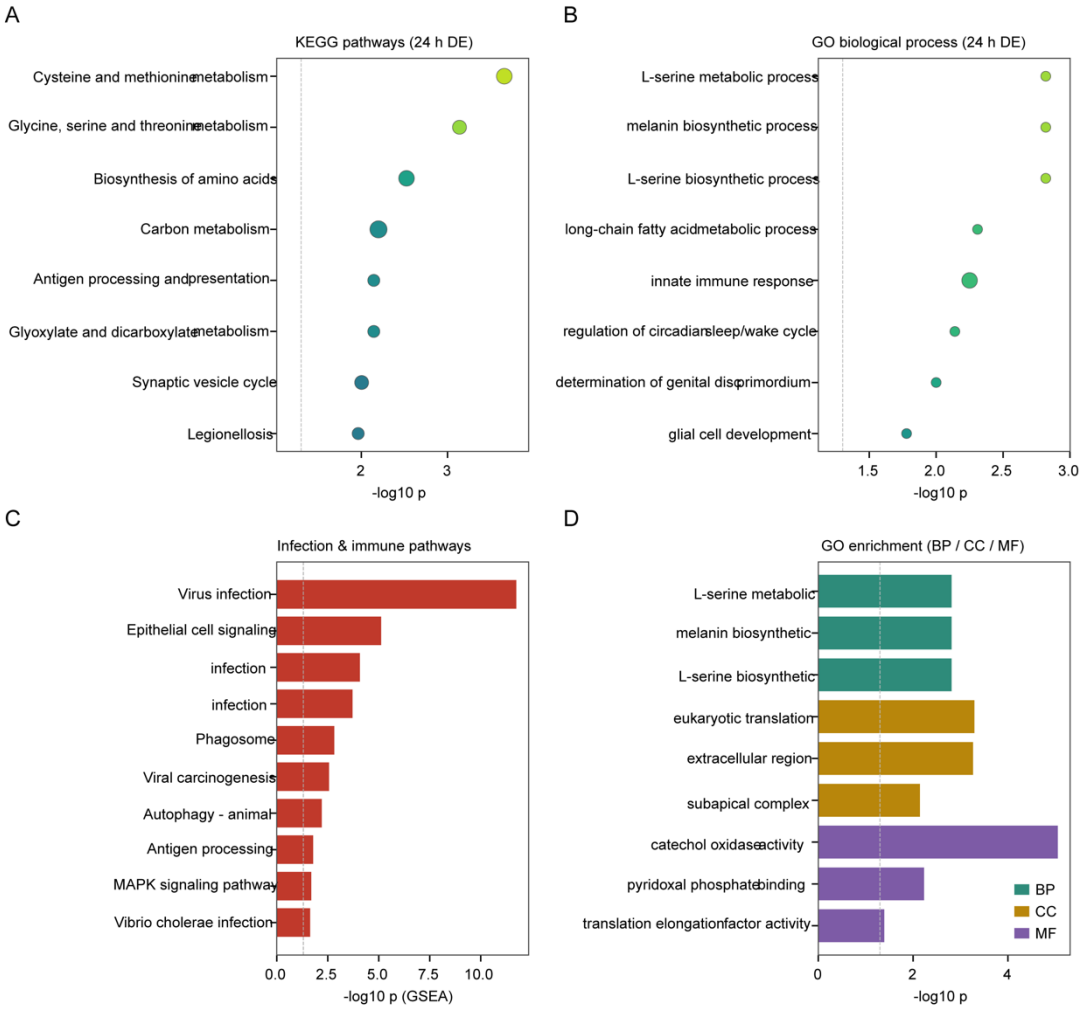

Fig. S3. Pathway and gene-set enrichment of the 24 h response. (A) KEGG pathway and (B) GO biological-process over-representation among 24 h DEGs (x, −log10 P; dot size, number of DE genes in the term; colour, adjusted P; dashed line, P = 0.05). (C) Rank-based gene-set enrichment of infection- and immunity-associated KEGG pathways (bar length, −log10 P; colour indicates direction, up in red or down in blue in Virus). (D) GO enrichment summarized across the Biological Process, Cellular Component and Molecular Function domains.

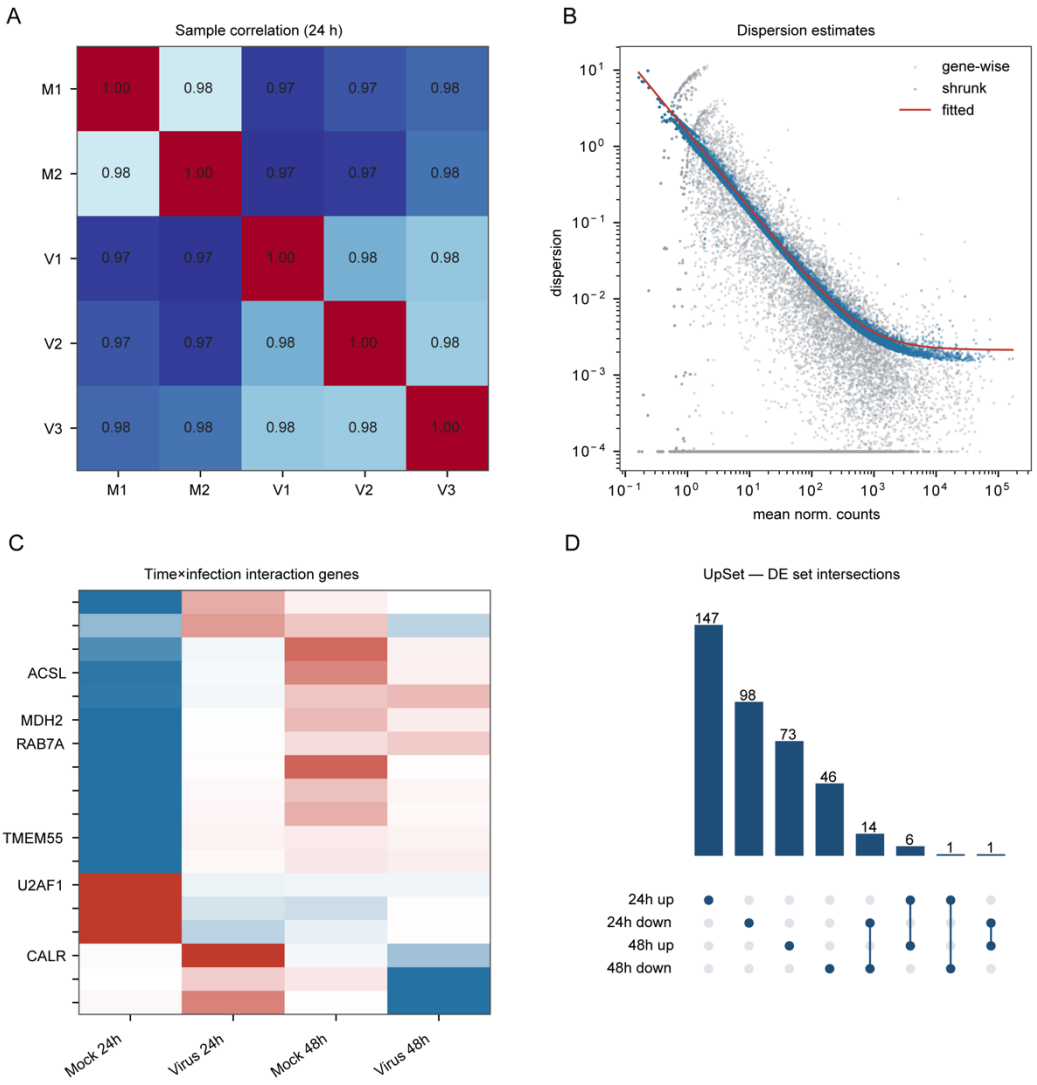

Fig. S4. Quality control and time × infection interaction. (A) Pairwise Pearson correlation of the 24 h libraries (log2-normalized counts). (B) Negative binomial dispersion estimates as a function of mean expression, showing gene-wise estimates, the fitted mean–dispersion trend and the empirical-Bayes-shrunken values. (C) Heatmap of the top time × infection interaction genes identified by the two-factor model (row z-scores averaged within the four conditions — Mock 24 h, Virus 24 h, Mock 48 h, Virus 48 h — and hierarchically clustered). (D) UpSet plot of the four DEG sets (24 h up/down, 48 h up/down) showing set sizes (top bars) and exclusive intersections (dot matrix).

Tables

Table S1. Cryo-EM data collection, refinement, and validation statistics.

	The subunit of AaTLV-IMCAS
Data collection and processing	
Voltage (kV)	300
Electron exposure ($e^-/Å^2$)	60
Defocus range (μm)	-1 to -2
Pixel size (Å)	0.97
Number of frames collected	*EER mode
Micrographs Collected (no.)	5,160
Symmetry imposed	I
Final particles (no.)	54,310
Map resolution (Å)	2.11
FSC threshold	0.143
Refinement	
Initial model used (PDB code)	AlphaFold3
Map sharpening methods	DeepEMhancer
Model composition	-
Non-hydrogen atoms	4,336
Protein residues	568
Ligands	-
R.m.s. deviations	
Bond lengths (Å)	0.003
Bond angles (°)	0.615
Validation	
MolProbity Score	1.01
Clash Score	1.61
Poor rotamers (%)	0.00
Ramachandran plot	
Favored (%)	97.51
Allowed (%)	2.49
Disallowed (%)	0.00

***** Electron-event representation (EER) mode generates data at a rate of 320 frames per second for a duration of 3 to 5 seconds.